Am J Cancer Res 2021;11(12):5965-5978
www.ajcr.us /ISSN:2156-6976/ajcr0138878

Original Article

RRM2 gene expression depends on BAF180 subunit of SWISNF chromatin remodeling complex and correlates with abundance of tumor infiltrating lymphocytes in ccRCC

Joanna Szarkowska[1*], Pawel Cwiek[2*], Michal Szymanski[3*], Natalia Rusetska[1], Iga Jancewicz[1], Malgorzata Stachowiak[1], Monika Swiatek[1], Maciej Luba[1], Ryszard Konopinski[1], Szymon Kubala[2], Renata Zub[1], Jakub Kucharz[4], Pawel Wiechno[4], Janusz A Siedlecki[5], Sergiusz Markowicz[1], Elzbieta Sarnowska[1#], Tomasz J Sarnowski[2#]

[1]Department of Experimental Immunotherapy, Maria Sklodowska-Curie National Research Institute of Oncology, Warsaw, Poland; [2]Institute of Biochemistry and Biophysics, Polish Academy of Sciences, Warsaw, Poland; [3]Department of Urology and Urological Oncology, Central Clinical Hospital of Ministry of the Interior and Administration in Warsaw, Warsaw, Poland; [4]Department of Uro-oncology, Maria Sklodowska-Curie National Research Institute of Oncology, Warsaw, Poland; [5]Department of Molecular and Translational Oncology, Maria Sklodowska-Curie National Research Institute of Oncology, Warsaw, Poland. [*]Equal contributors. [#]Equal contributors.

Received September 4, 2021; Accepted October 12, 2021; Epub December 15, 2021; Published December 30, 2021

Abstract: About 40% of clear cell renal cell carcinoma (ccRCC) cases carry the *pbrm1* mutation inactivating BAF180 subunit of the SWI/SNF chromatin remodeling complex (CRC). Here we show that the majority of transcriptomic changes appear at the stage I of ccRCC development. By contrast, the stage II ccRCC exhibits hyperactivation of DNA replication demonstrated by the overexpression of several genes, e.g., *RRM1* and *RRM2* genes encoding subunits of ribonucleotide reductase (RNR) complex. We found that the degree of *RRM1* and *RRM2* upregulation in ccRCC patients depends on *pbrm1* mutation. We show that the BAF180 protein product of the *PBRM1* gene directly binds to *RRM1* and *RRM2 loci*. The BAF180 binding regions are targeted by regulatory proteins previously reported as SWI/SNF CRC interacting partners. BAF180 binding to *RRMs loci* correlates with enrichment of H3K27me3 in case of *RRM1* and H3K14Ac on *RRM2*, indicating the existence of differential regulatory mechanism controlling expression of these genes. We found that the strong overexpression of RRM2 in ccRCC patient samples correlates with T cell infiltration. Surprisingly, the majority of tumor infiltrating lymphocytes (TILs) consisted of $CD4^+$ T cells. Furthermore, we show that exhausted $CD4^+$ T cells induced the expression of the *RRM2* gene in the primary ccRCC cell line. Collectively, our results provide the link between *PBRM1* loss, RRM2 expression and T cell infiltration, which may lead to the establishment of new treatment of this disease.

Keywords: Clear cell renal cell carcinoma, BAF180, SWI/SNF, RRM, $CD4^+$ T cell, T cell exhaustion

Introduction

Renal cancers (RCCs) represent 2-3% of all malignancies in adults [1, 2]. Approximately 75% of all RCC cases are classified as clear cell renal cell carcinoma (ccRCC) [3-5]. ccRCC is characterized by strong metabolic alterations leading to glycogen and fatty acids accumulation in cancer cells [3, 6].

Approximately 90% of ccRCC cases carry the *VHL* (*Von Hippel Lindau*) mutations [7, 8], while 40% carry mutations inactivating *PBRM1* gene encoding BAF180 subunit of SWI/SNF (SWITCH/Sucrose Non-Fermenting) chromatin remodeling complex (CRC). SWI/SNF CRC is reported to be frequently mutated and/or affected in various cancer types [9, 10] including ccRCC [7]. The transcript profiling study identified several key genes involved in ccRCC metastasis, e.g., *Ribonucleotide Reductase M2 (RRM2)* [11], which is a subunit of ribonucleotide reductase (RNR) complex. The RNR complex is also frequently mutated in various cancer types [11].

Table 1. Sequences of primers used for qRT-PCR

Primer	Forward	Reverse
UBIQUITIN	ATTTGGGTCGCGGTTCTTG	TGCCTTGACATTCTCGATGGT
RRM1	CACCAGCAAAGATGAGGTTGC	GGGGCGATGGCGTTTATTTG
RRM2	CACGGAGCCGAAAACTAAAGC	TCTGCCTTCTTATACATCTGCCA
RRM2B	CCTTGCGATGGATAGCAGATAGA	AGTCCTGGCATAAGACCTCTC
BAF180	TGATGGCCAACAAGTACCAA	AGATCAAAGACTCCGGCTCA

RNR is an enzyme catalyzing the reduction of ribonucleotides (NDPs) to deoxyribonucleotides (dNDPs) to maintain optimal level of dNTPs, which are further used for DNA replication or repair [12, 13]. The mammalian RNR holoenzyme consists of RRM1-large catalytic subunit and a small subunit, essential for catalysis of the reaction-RRM2 or RRM2B homodimer, respectively [12, 14]. The aberration in RNR subunits leads to the nucleotide imbalance, replication stress and genome instability as well as increased mutation rates thus promotes carcinogenesis [15-17]. RRM2 inhibition in RCC lines results in the cancer cells' growth arrest *via* attenuation of the dNTPs pool [18].

Here, we show that the most of global transcriptomic changes appear at the early stage of the ccRCC development, while the stage II ccRCC exhibits upregulation of DNA replication-related genes, including *RRM1* and *RRM2* coding for subunits of the RNR complex. Moreover, we demonstrate that *RRM1* and *RRM2* promoter regions are directly targeted by the BAF180 subunit of SWI/SNF CRC, and the *RRM1* and *RRM2* expression depends on the presence of functional BAF180. Consequently, the RRM2 overaccumulation was observed in some ccRCC cells in patient samples. This overaccumulation correlated with T cell infiltration. Furthermore, the increased RRM2 protein level was observed in the primary ccRCC cell line co-cultivated with persistently activated $CD4^+$ T cells which undergo exhaustion. Collectively, our results give a new insight into BAF180 function and the effects of *PBRM1* mutation on ccRCC development and treatment.

Materials and methods

Transcript profiling

The microarray datasets obtained from Gene Omnibus Database (GEO), GSE6344 [19], and GEO (GSE36895) [20] were reanalyzed using GeneSpring GX software (Agilent) according to the guided workflow or advanced guided protocol with 1.45 fold change. All normal kidney cortex samples were normalized and treated as normal (control sample), and all ccRCC samples as cancer sample.

Statistical analysis

Statistical analyzes were performed using GraphPad Prism 5.0 software. Shapiro-Wilk normality test, paired t-test, Chi-square, Pearson correlation, Mann-Whitney rank test for independent samples were used. *P* value <0.05 was considered as statistically significant. Cox Proportional Hazard regression was used to estimate the relationship between the gene expression and survival rate using the SurvExpress platform. Two risk groups were generated using the prognostic index median. The Log-rank test was used to evaluate the equality of survival curves [21].

Cell culture

Human A498 and 786-O ccRCC cell lines were authenticated at Leibniz Institute DSMZ-German Collection of Microorganisms and Cell Cultures. A498 and 786-O were cultured in RPMI 1640 (Biowest) or RPMI 1640 ATCC-modified (Gibco), respectively. Cells were cultured without antibiotics in a humidified atmosphere with 5% CO_2 at 37°C.

RNA isolation and RT-qPCR analysis

Total RNA from fresh cancer and healthy tissue was purified using ReliaPrep™ Kit (Promega). 1 µg of total RNA was used for cDNA synthesis. Reverse transcription was performed with Transcriptor First Strand cDNA Synthesis Kit (Roche). For the RT-qPCR iQ™ SYBR© Green Supermix (Bio-Rad) was used, and data were calculated using the $2^{-\Delta\Delta CT}$ method with ubiquitin (UBC) as internal control. Primers used in this study are summarized in **Table 1**.

Western blot analysis

A total protein extracts from snap-frozen tumor and healthy tissues or 10^6 cells of 786-O primary renal cancer cell line were subjected to Western blot analysis with anti-PBRM/BAF180 (1:1000, CST, #91894) antibody diluted in 5% bovine fetal albumin and anti-RRM2 (1:1000,

Table 2. Sequences of primers used for chromatin immunoprecipitation

Primer	Sequence forward	Sequence reverse
RRM1-3	TCTCGAACTCCTGACCTCGT	CCAGGCTCCCTGTGAAGTAA
RRM1-4	GAGGGCAGTGAGAAACCAAC	CCTTGTGGAGGTAGGATGGA
RRM1-5	GCTCTGATTTGCGTCAGGAT	GGAGGAAAGGCGGTTAATTT
RRM1-6	AGCGGGCTCTAGGTGCTAC	AGACTGACAGGCGACGTGTA
RRM2-3	TGCTCAGTTTGCAATTAAAACAA	ACCCTTGCCTTAAGAATTGC
RRM2-4	GCCATGTCCCGTAGTTTGAA	AAGCGACCAGGCTTCTTACA
RRM2-6	AGCCTGGGTAGGGGCAAG	GACACGGAGGGAGAGCATAG

CST, #65939) diluted in 5% non-fat dry milk. The proteins were extracted using urea buffer and separated by SDS-PAGE gel electrophoresis (the acrylamide concentration was 10% in resolving gel and 5% in stacking gel). The goat anti-rabbit (1:10000 CST, #7074) conjugated with HRP was used as a secondary antibody. The Western blot signal was visualized using the WesternBright™ Quantum detection kit (Advansta). For loading control, the stain-free method (0.5% TCE) was used.

Immunohistochemistry

Immunohistochemistry (IHC) analysis was performed on 4-μm tissue sections from paraffin embedded tumor samples using the EnVision FLEX+ kit (Dako, Glostrup, Denmark) according to the protocol. Anti-PBRM/BAF180 (CST, #91894) in dilution 1:50, anti-RRM2 (CST, #65939, 1:200), anti-CD8 (CST, #85336, 1:200) and anti-CD4 (Abcam, ab133616, 1:500) were used as primary antibodies. The IHC reaction was developed with substrate-3,3'-diaminobenzidine tetrahydrochloride (Dako). One minute hematoxylin counterstaining was performed for nuclear contrast. The intensity and percentage of staining cells were calculated using the H-score method.

Chromatin immunoprecipitation (ChIP)

Chromatin was immunoprecipitated from 3×10^6 A498 cells crosslinked with 1 mM Bis-(sulfosuccinimidyl) glutarate and 1% formaldehyde according to the protocol [22] with some modifications. Briefly, isolated chromatin was broken into 100-500 bp fragments by sonication (Bioruptor UCD-200) for five cycles (the 30 s on/30 s off, 320 W, 4°C). Between each cycle of sonication, samples were incubated on ice for 5 min. After sonication, each sample was treated with RNase (125 μg/mL, Thermo Scientific) for 15 min on ice, followed by centrifugation (10 min, 13,800 RPM, 4°C). The collected supernatant was diluted four times with wash buffer. Such prepared chromatin was incubated O/N at 4°C with the following antibodies: anti-PBRM1/BAF180 (CST, #91894), anti-H3 (Abcam, ab17-91), anti-H3K27me3 (CST, #9733) and anti-H3K14Ac (Millipore, 07-353) and as a mock control Normal Rabbit IgG (CST, #2729). The recovery ratio of immunoprecipitated DNA relative to IgG DNA was measured by qPCR and calculated using $2^{-\Delta\Delta Ct}$ method [23]. Primers used for ChIP-qPCR analysis are listed in **Table 2**.

$CD4^+$ T cell isolation, activation and co-culture

$CD4^+$ T cells were isolated from healthy donor whole blood samples and activated polyclonally for 12 days, according to [24]. Briefly, the ficoll method for mononuclear blood cell isolation was employed. Subsequently, the Dynabeads™ Regulatory $CD4^+/CD25^+$ Cell Kit (Invitrogen, 11363D) and the Activation/Expression Kit (Miltenyi Biotec) were used for isolation and activation of $CD4^+$ T cells. Further, $CD4^+$ T cells were cultured in AIM V™ medium (Gibco) with 10 U/ml interleukin-2 (R&D Systems) for 12 days in standard conditions. After 12 days, polyclonally activated $CD4^+$ T cells were subsequently restimulated polyclonally for the next 3 days and co-cultured with 786-0 cells in RPMI 1640 medium without supplementation with exogenous IL-2. 786-0 cells were seeded onto a T-75 bottle near confluency one day before co-culture start. After 3 days of co-culture, cancer cells were separated from T cells and collected for further analysis. The 786-0 cells cultured without $CD4^+$ T cells were used as a control cell line.

ccRCC patient characteristics

We retrospectively analyzed snap frozen and formalin-fixed, paraffin-embedded samples from 20 patients diagnosed with ccRCC between January 2013 and December 2016 in the Maria Sklodowska-Curie National Research Institute of Oncology in Warsaw. The detailed patients' characteristic is described in **Table 3**.

Table 3. Patient characteristics

Characteristics	n (%)
Gender	
Female	8 (40%)
Male	12 (60%)
Age	
<60	4 (20%)
≥60	16 (80%)
Fuhrman grade[a]	
G1	0 (0%)
G2	9 (45%)
G3	11 (55%)
G4	0 (0%)
pT category[b]	
pT1	9 (45%)
pT2	2 (10%)
pT3	7 (35%)
pT4	1
Metastasis	
no metastasis	12 (60%)
Metastasis	8 (40%)
Female	3 (37.5% of total metastasis)
Male	5 (66.5% of total metastasis)

a, based on Fuhrman grade classification; b, according to pTNM classification.

Results

Stage I and stage II ccRCC exhibit common and differential transcriptomic changes

The reanalysis of GSE6344 datasets representing stage I ccRCC and stage II ccRCC indicated that 3700 genes were misregulated in ccRCC samples comparing to healthy control. 1577 differentially expressed genes were specific to stage I, while 445 genes were specific to ccRCC stage II. Both ccRCC stages shared 1678 common differentially expressed genes (**Figure 1A**), indicating that main transcriptomic changes in ccRCC appear already at the very beginning of the disease. In-depth analysis revealed that 1602 genes were downregulated in both stages, although 693 were specific to stage I and 185 genes were stage II specific. 724 downregulated genes were common for both stages. The Gene Ontology (GO) analysis indicated that downregulated genes in stage I are related to metabolic processes, cell differentiation, development, and morphogenesis. Interestingly, among genes specifically downregulated in stage II, only one GO class (cellular response to oxygen-containing compound) was enriched (**Figure 1B**). A total of 2098 genes were upregulated in both stages, of which 937 genes were commonly overexpressed in both stages, while 901 were characteristic for stage I and 260 were specific for stage II of ccRCC. Among genes overexpressed specifically in the stage I, the GO classes related mainly to general processes were enriched (**Figure 1C**). Interestingly, among genes specifically upregulated in ccRCC stage II only one GO category, DNA replication, was found. Following genes *RRM1, KIAA0101, BARD1, ATR, CDK1, FEN1, MCM6, RTFDC1, RRM2, MCM2, DONSON, ORC5, DTL, PCNA,* and *JUN* were assigned to the aforementioned category (**Figure 1C**). Interestingly, the expression of *RRM1* and *RRM2* genes encoding main subunits of the RNR enzyme was strongly upregulated in the stage II ccRCC.

The expression of RRM1, RRM2, and RRM2B genes is affected in ccRCC

The *VHL*, *BAP1,* and *PBRM1* genes are listed as the most frequently mutated in ccRCC [25]. Thus, to verify the results coming from our global analyses using datasets corresponding to particular patients, we reanalyzed GSE36895 datasets representing 29 ccRCC and 24 normal kidney cortex samples with known *VHL*, *BAP1,* and *PBRM1* mutation status [20]. In this analysis, we focused on *RRM1*, *RRM2,* and *RRM2B* genes encoding subunits of the RNR complex responsible for maintaining the proper level of dNTPs. This analysis indicated statistically significant overexpression of *RRM1*, *RRM2,* and *RRM2B* genes in cancer samples comparing to healthy tissues (**Figure 2A-C**), however, the significance for *RRM2B* gene was lower than for other *RRM* genes. Consistently, the analysis performed on TCGA datasets using Ualcan (http://ualcan.path.uab.edu/) [25] indicated that the *RRM2* gene is the most significantly overexpressed *RRM* family gene in ccRCC samples comparing to the normal kidney. Further analysis revealed that *RRM1* and *RRM2* overexpression is independent on Fuhrman grade (FG) (**Figure 2D**, **2E**). By contrast, the *RRM2B* gene was slightly overexpressed only in samples corresponding to FG1-2 (**Figure 2F**). Of note, FG is related to the

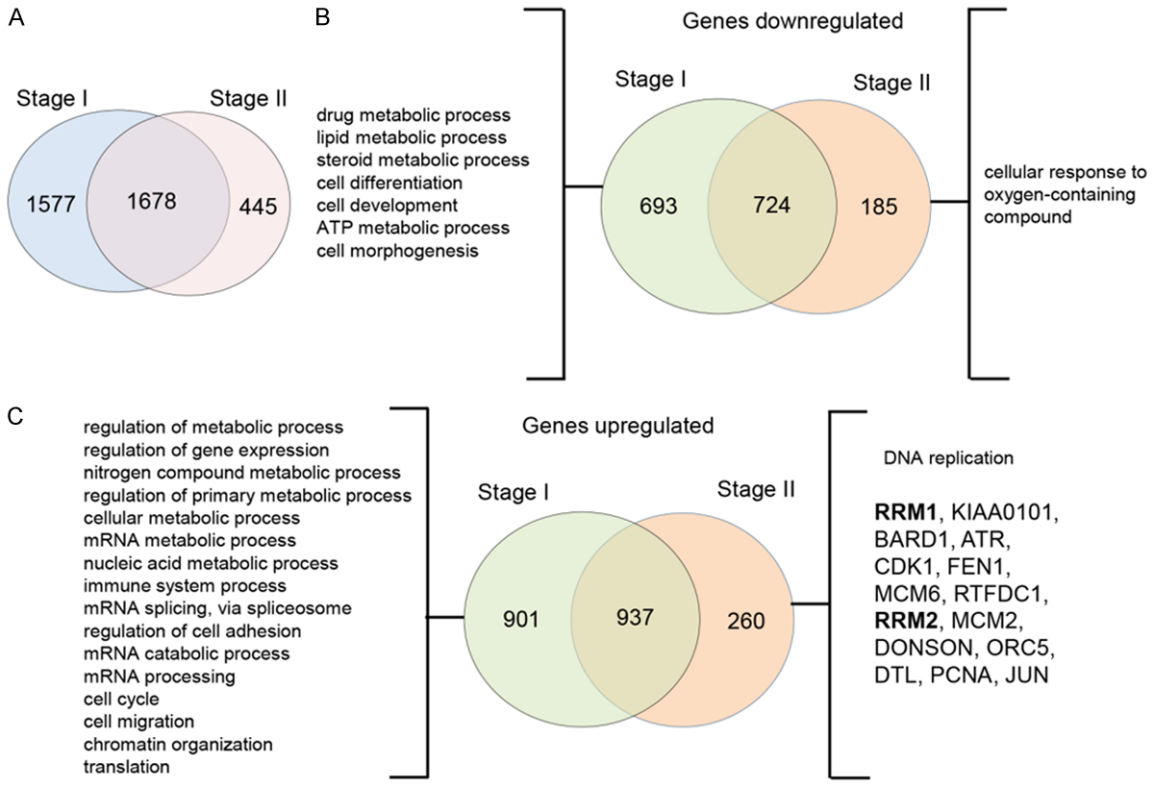

Figure 1. ccRCC exhibits characteristic transcriptomic changes. (A) Genes commonly and differentially deregulated in stage I and stage II ccRCC. (B) Genes and processes downregulated and (C) upregulated in ccRCC stage I and stage II.

stage of the disease and prognosis for patients [26]. The overexpression of *RRM1* and *RRM2* genes was independent on the patients' gender (**Figure 2G**, **2H**). The *RRM2B* overexpression is gender indivisible (**Figure 2I**). We observed the statistically significant *RRM2B* overexpression when the FG and gender were combined, although the statistical power was lower than in the case of other *RRMs* (**Figure 2C**).

Moreover, *RRM1*, *RRM2,* and *RRM2B* expression profiles relevantly correlated with patients' survival rates (**Figure 3A**). The survival analysis indicated that ccRCC patients with strong *RRM2* overexpression had lower survival rates (**Figure 3B**). Additionally, the expression profiling of all *RRM* genes indicated the strongest overexpression of the *RRM2* gene in almost all tumor samples comparing to normal tissues (**Figure 3C**). Thus, this observation strongly suggests that *RRM2* overexpression may be crucial for ccRCC development and progression.

BAF180 directly regulates expression of RRM1 and RRM2 genes

PBRM1 gene encoding BAF180 protein is commonly mutated in ccRCC. BAF180 is a subunit of SWI/SNF CRC which is known as a global regulator of transcription. Indeed, the analysis of GSE36895 datasets indicated that *RRM1* and *RRM2* expression depends on the presence of *PBRM1* mutations inactivating the BAF180 subunit of SWI/SNF CRC. The highest expression of *RRM1* was found only in cancer cells without mutated *PBRM1* (**Figure 4A**).

Cognately to *RRM1*, the expression level of *RRM2* in ccRCC increased far more when no mutations in *PBRM1* were detected (**Figure 4B**). Thus, we analyzed eight ccRCC patient samples for the presence of BAF180 protein (detected by Western blot using anti-BAF180 antibody). We detected a complete lack of BAF180 in three tumor samples (patient #1, 5, and 6). In one sample, we could detect only traces of BAF180 (patient #3). In four tumor

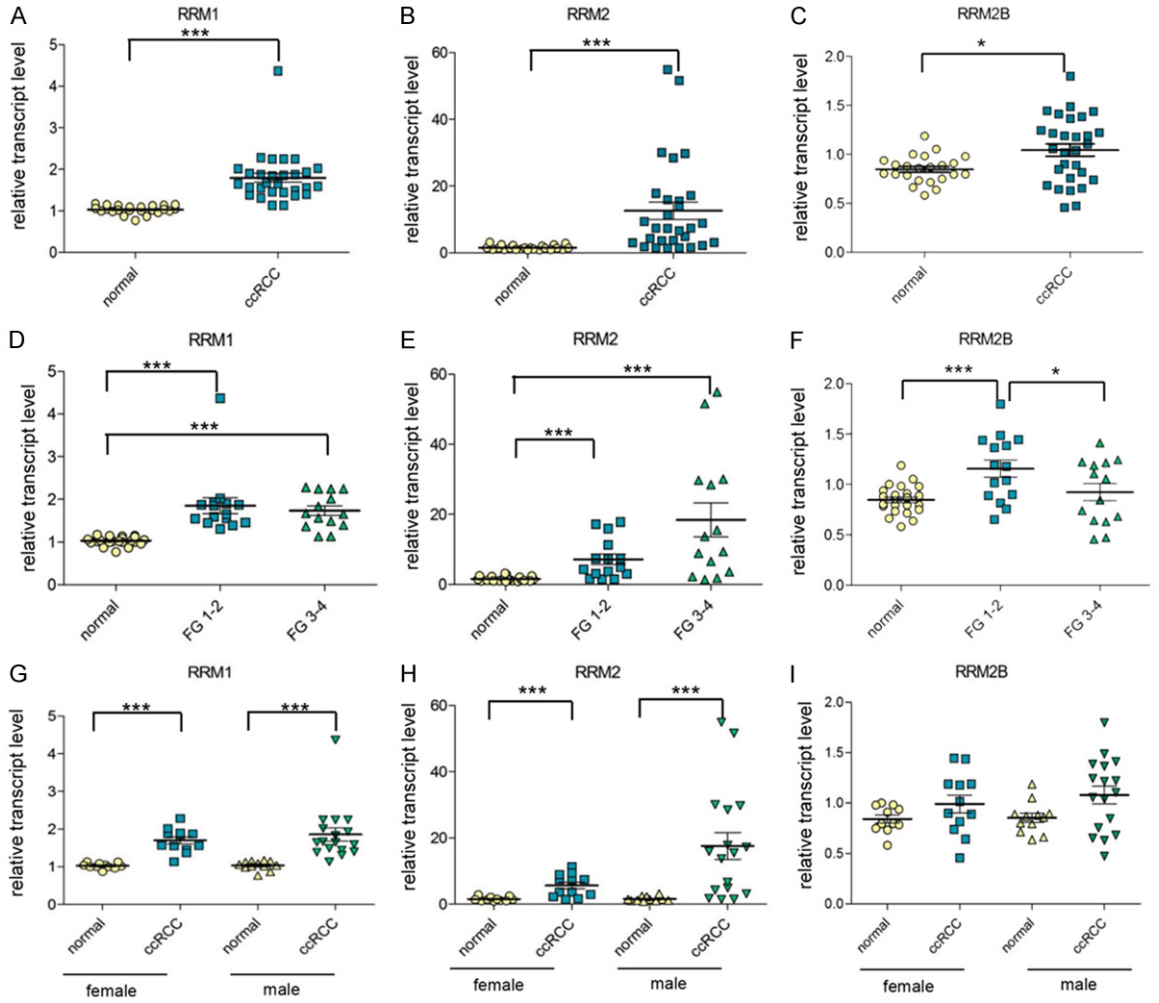

Figure 2. *RRM* family genes are deregulated in ccRCC. Comparison of (A) *RRM1*, (B) *RRM2* and (C) *RRM2B* genes expression in ccRCC samples *vs* healthy kidney tissue. Comparative analysis of (D) *RRM1*, (E) *RRM2* and (F) *RRM2B* expression dependent on ccRCC Fuhrman grade. Analysis of (G) *RRM1*, (H) *RRM2* and (I) *RRM2B* expression regarding patients gender. *P* value <0.05 was considered as statistically significant, *P<0.05, **P<0.001, ***P<0.0001.

samples (patient #2, 4, 7, 8) we detected the presence of BAF180 protein, however the protein levels substantially differed between tested samples (**Figure 4C**). Subsequently, we analyzed the transcript levels of *RRMs* and *PBRM1* (BAF180) genes (**Figure 4D**) in these particular samples. The tumor samples were characterized by various levels of *PBRM1* transcript, which in some cases did not corelate to the BAF180 protein level. The likely explanation of this phenomenon could be the presence of mutations in the *PBRM1* gene, which might affect or prevent the detection of BAF180 protein by anti-BAF180 antibodies. Thus, we could not exclude the existence of mutated BAF180 protein with partially retained function or even gain-of-function BAF180 in analyzed samples assessed as BAF180-depleted.

On the other hand, the high *PBRM1* transcript level was correlating with the increased expression level of *RRM* genes. In samples with a lower abundance of *PBRM1* transcript, the transcript levels of all tested *RRM* genes were significantly decreased in comparison to samples characterized by *PBRM1* transcript accumulation. Collectively, this observation provided the hint that the functional BAF180 protein may be involved in the control of *RRMs* expression (**Figure 4D**).

Therefore, we decided to check the ability of BAF180 to bind the *RRM1* and *RRM2* promoter

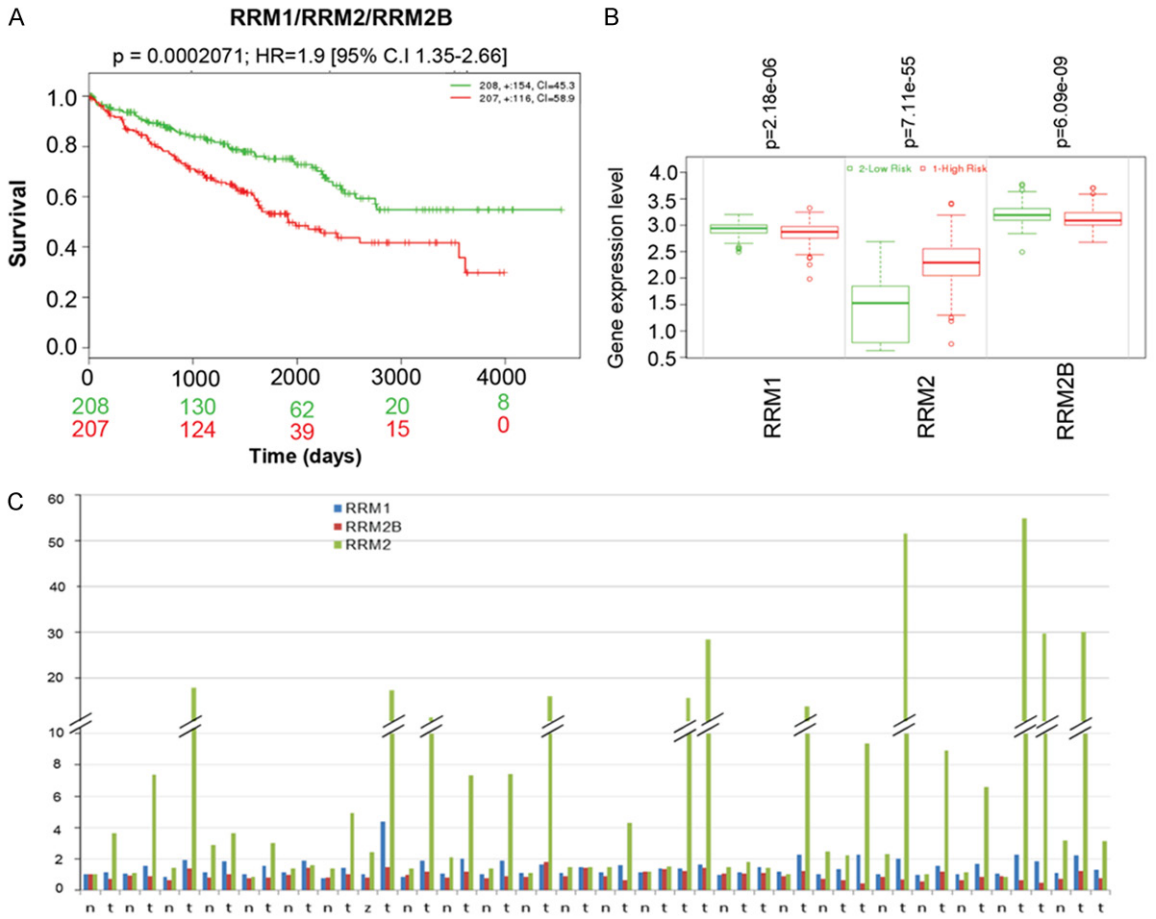

Figure 3. Deregulation of *RRM* expression correlates with patient characteristics and survival prediction. A. Survival analysis of ccRCC patient depending on *RRM1*, *RRM2* and *RRM2B* expression status, P=0.0002071; HR=1.9 [95% CI 1.35-2.66]. B. Expression of *RRM1*, *RRM2* and *RRM2B* genes differentially correlates with mortality risk. A and B. Based on TCGA KIRC database. C. The expression level of *RRM1*, *RRM2* and *RRM2B* differs between particular normal and corresponding tumor patient samples. *P* value <0.05 was considered as statistically significant.

regions directly, using the chromatin immunoprecipitation (ChIP) approach. As the A498, 786-O and CAKI-1 cell lines express the wild-type BAF180 protein, we chose the A498 cell line for the chromatin immunoprecipitation analysis. The ChIP-qPCR analysis revealed BAF180 binding to the promoter region of the *RRM1* gene in position ~-810 bp, ~-300 bp, and ~-40 bp upstream of the first transcription start site (TSS1) (**Figure 5A**). The BAF180 binding to *RRM1 locus* at the position ~-300 bp upstream of TSS1 correlated with enhanced nucleosome occupancy (**Figure 5B**) demonstrated by the enrichment of DNA fragments in ChIP with antibodies specifically recognizing histone 3 (H3). Furthermore, the analysis of the occupancy of the *RRM1* promoter region by H3 with trimethylated lysine 27 (H3K27me3) revealed enrichment around the TSS1/TSS2 region, while the acetylated H3 (H3K14Ac) was not detected (**Figure 5C**), together indicating the possible regulatory events appearing on the *RRM1 locus* (**Figure 5D**).

The binding of BAF180 was observed in the promoter region of *RRM2* gene ~-610 bp from the first TSS and ~+140 bp downstream of TSS1 in a place where alternative *RRM2* TSS2 was recognized (**Figure 5E**). The analysis of H3 positioning on the *RRM2 locus* revealed the ~3.5-fold enrichment at the position ~-850 bp from TSS1 and discrete enrichment (~1.5-fold) around the +150 bp downstream of TSS1. Of note, no significant enrichment in the position around -610 bp upstream of TSS1, representing one of the BAF180-target regions at the *RRM2* promoter (**Figure 5F**) was observed. Consistently, we found ~3-fold enrichment of

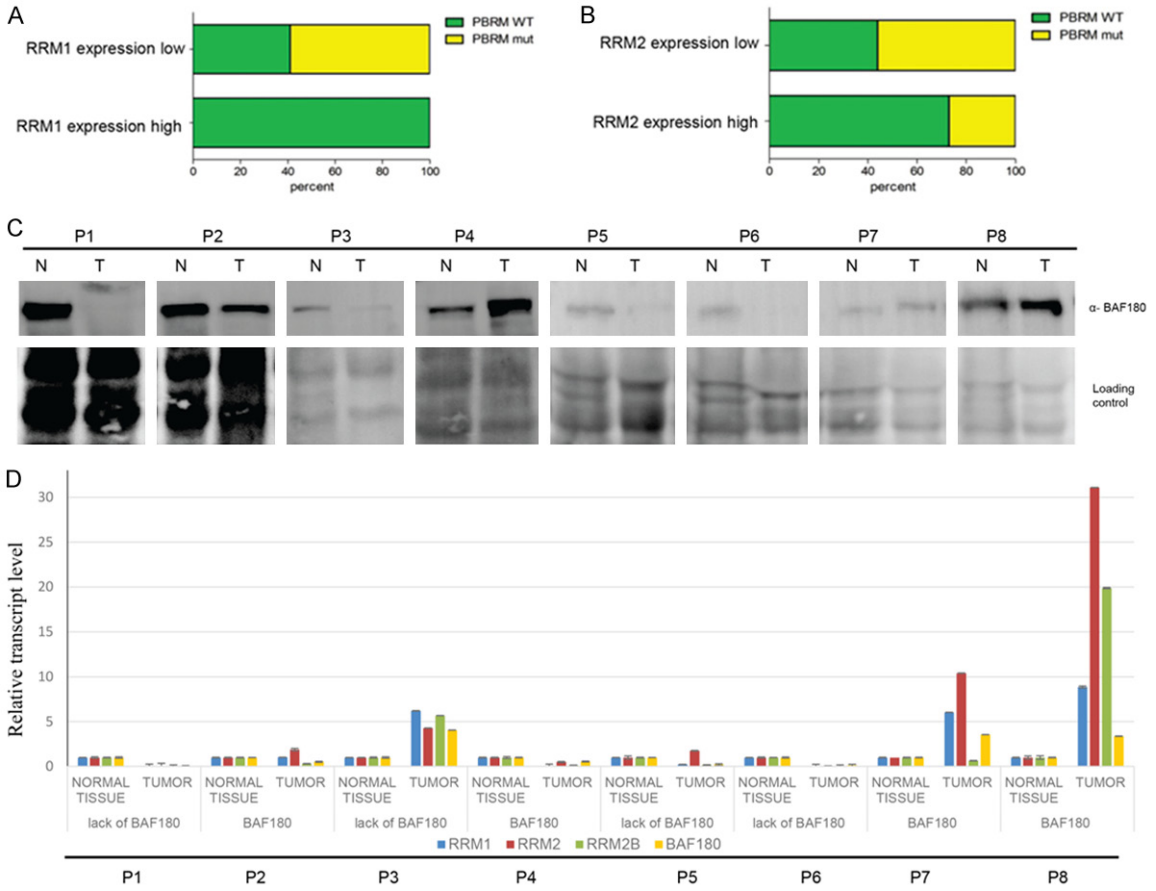

Figure 4. The presence of *pbrm1* mutation inactivating BAF180 subunit of SWI/SNF CRC correlates with the expression of RRM genes. A. The presence of wild type PBRM1 is associated with stronger RRM1 expression. B. The presence of wild type PBRM1 is associated with stronger RRM2 expression. C. ccRCC is frequently characterized by the significant decrease or loss of BAF180 protein. P: patient, N: normal tissue, T: tumor. D. The RRMs genes expression levels correlate with the expression of PBRM1 gene encoding BAF180 protein. The ubiquitin was used as an internal control. The data is normalized to normal, healthy tissue in each tumor-normal tissue pair.

H3K14Ac in the position ~-610 bp from TSS1, while the enrichment of H3K27me3 was not found at the *RRM2* promoter region (**Figure 5G**).

The precise investigation of *RRM1* and *RRM2* promoter regions for the presence of *cis*-regulatory elements using the Transfac database indicated that the TSS1/TSS2 position on the *RRM1* promoter region may be targeted by HDAC1, HDAC2, EP300, BRCA1, and MYC regulatory proteins (**Figure 5D**), while the *RRM2* promoter region corresponding to BAF180 target domains around TSS1/TSS2 may be potentially recognized by HDAC1, HDAC2, EP300, BRCA1, E2F6 proteins. Additionally, the MYC transcription factor targeted the *RRM2* promoter region next to the second BAF180 target site (**Figure 5H**). Interestingly, the detected transcription factors were reported as direct partners of SWI/SNF CRCs [10, 27, 28]. Together, our results indicate the existence of potentially distinct regulatory mechanisms controlling the expression of *RRM1* and *RRM2* genes (**Figure 5D**, **5H**).

The RRM2 expression correlates with tumor infiltrating lymphocyte abundance

The IHC analysis for RRM2 protein abundance in patient samples revealed the strong, ectopic RRM2 expression in some cancer cells. Surprisingly, we observed the high TILs infiltration nearby these cells (**Figure 6A**). To identify which T cell class infiltrates the tumor in ccRCC patient samples, we performed IHC analysis using anti-CD8 and anti-CD4 antibodies. Interestingly, the $CD4^+$ T cell abundance was

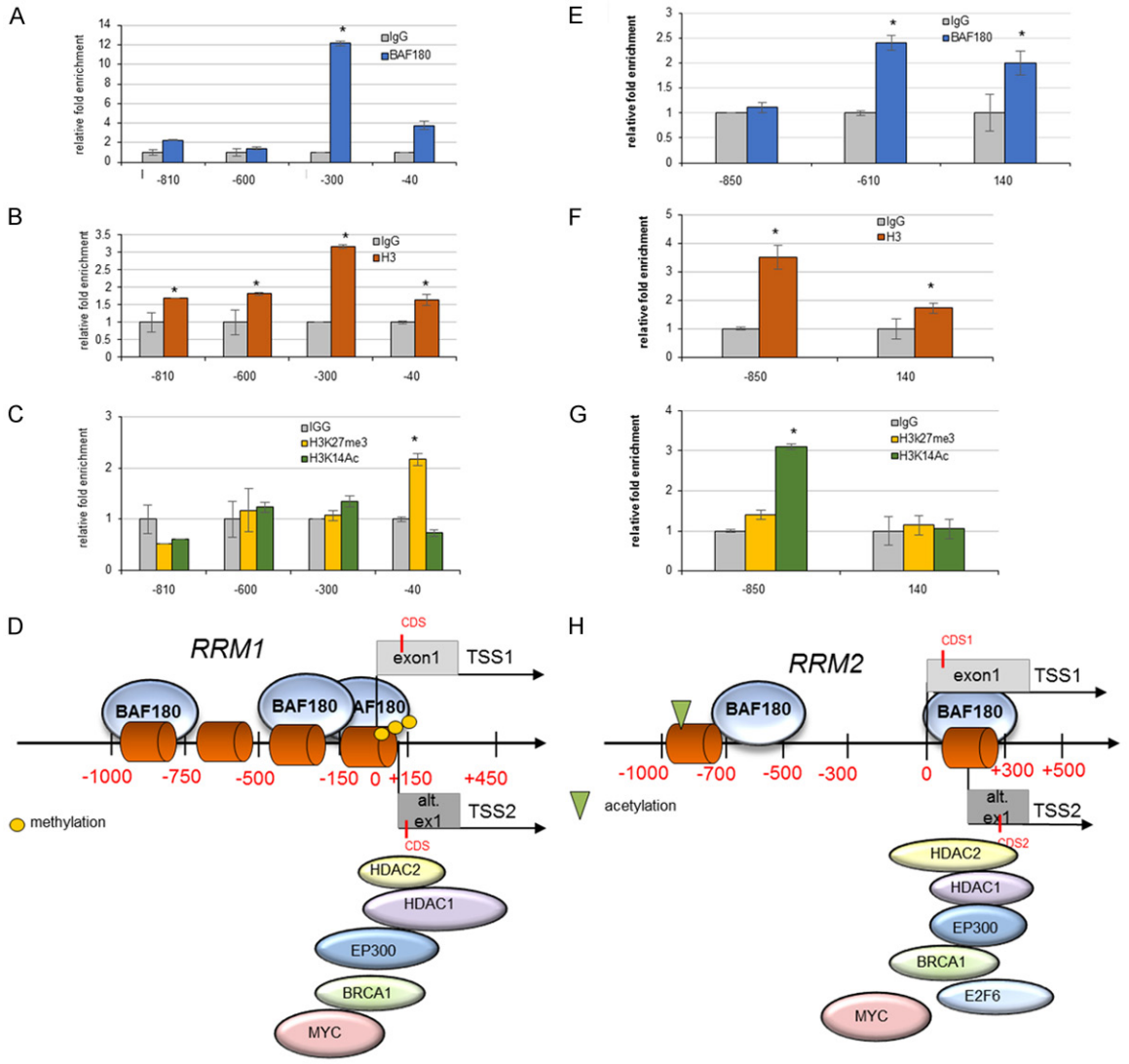

Figure 5. BAF180 binds to *RRM1* and *RRM2* promoter regions. The ChIP analysis for (A) BAF180 abundance, (B) histone H3 positioning and (C) histone marks H3K27me3, H3K14Ac on *RRM1* gene promoter region. (D) The schematic overview of chromatin status on *RRM1* promoter region. The binding of (E) BAF180, (F) histone H3 positioning and (G) histone marks H3K27me3, H3K14Ac on the *RRM2* gene promoter region. (H) The schematic representation of chromatin status on the *RRM2* promoter region. Black numbers correspond to the amplicon used in analyses. In (A-C, E-G) the values represent the middle of amplicon. The numbers in bracket represent number of amplicons for *RRM1* -810 bp (3), -600 bp (4), -300 bp (5), -40 bp (6); for *RRM2*-850 bp (3), -610 bp (4), 140 (6). The experiments were performed in three independent replicates. Asterisks indicate the statistically significant enrichment P<0.005.

significantly higher than that of $CD8^+$ T cells (**Figure 6B** and **6C**). The expression of CD4, known for being a marker of $CD4^+$ T cells positively correlated with RRM2 protein presence in ccRCC samples. According to [24], *RRM2* was downregulated in exhausted $CD4^+$ T cells, suggesting that *RRM2* elevated expression in ccRCC samples was originated in cancer cells but not in $CD4^+$ T cells (**Figure 6D**). We previously found that persistent, polyclonal activation of $CD4^+$ T cells for 12 days and subsequent restimulation for 3 days in the presence of 786-O cancer cells accelerated the exhaustion of $CD4^+$ T cells [24]. Here, we show the strong elevation of RRM2 protein level in 786-O cells co-cultured with persistently activated $CD4^+$ T cells undergoing exhaustion, in comparison to 786-O cells grown without T cells, suggesting $CD4^+$ T cell-dependent induction of RRM2 expression in cancer cells (**Figure 6E**). By con-

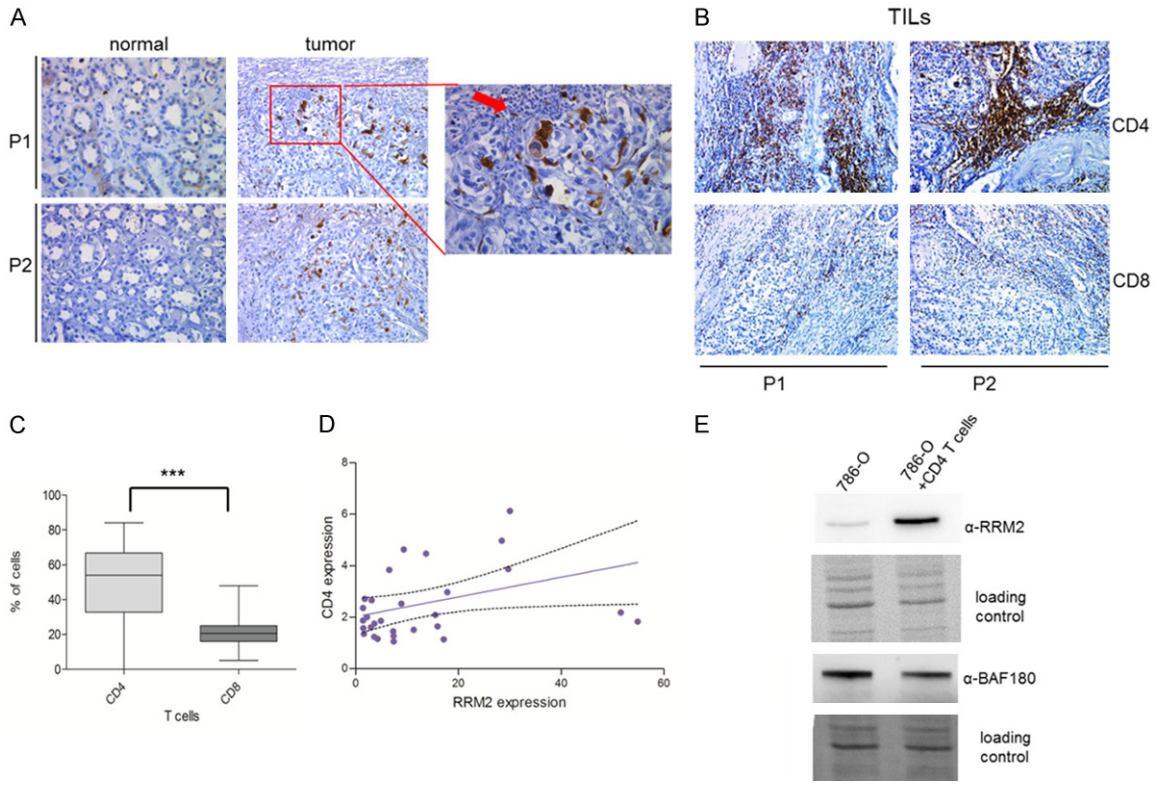

Figure 6. RRM2 expression correlates with CD4⁺ T cell infiltration in ccRCC samples. A. Strong staining for RRM2 is observed in single cells in the tumor area, and correlates with lymphocyte infiltration. The red arrow indicates TIL presence. B. The TILs in ccRCC are dominantly CD4⁺ but not CD8⁺. C. The percent of CD4⁺ TILs is statistically much higher than that of CD8⁺ TILs in patient samples; P<0.0001. D. CD4 expression level positively correlates with RRM2 expression in ccRCC samples; P<0.05. E. The RRM2 level increased in 786-O ccRCC cells due to their co-cultivation with persistently activated CD4⁺ T cells.

trast, the level of BAF180 in 786-O cells was not affected by their co-cultivation with CD4⁺ T cells (**Figure 6E**).

Discussion

The ccRCC is one of the most unpredictable cancer types. The transcript profiling analysis revealed that the most pronounced global transcriptomic changes, including, i.e., metabolism, kinase activity, RNA splicing, appear in the very early phase (stage I) of the ccRCC development. The proliferative potential and DNA replication efficiency of cancer cells (stage II) increase *via* upregulation of RNR encoding genes (*RRM1*, *RRM2, RRM2B*), which is in line with the significant association of the *RRM2* expression level with overall survival and recurrence-free survival rates in ccRCC patients [11]. The analysis of transcriptomic changes revealed the significant overexpression of *RRM1* in ccRCC tissues independently on FG and gender. A similar effect was observed for *RRM2*, although the *RRM2* level was even higher in more advanced ccRCC (FG3-4).

Interestingly, it was proven that the additional RNR subunit, the RRM2B protein, which may substitute the RRM2 in the RNR enzyme, is upregulated predominantly in low grade ccRCC (FG1-2). Moreover, the main factor affecting the survival curves of ccRCC patients was the *RRM2* gene overexpression. Patients with *RRM2* overexpression have a statistically significant decrease of survival rate consistent with previous findings that *RRM2* overexpression may be associated with higher tumor grade. The comprehensive transcriptomic analysis of *RRM1*, *RRM2,* and *RRM2B* expression in ccRCC and corresponding healthy tissue indicated the *RRM2* as a main RNR enzyme subunit that is strongly overexpressed in this cancer type. Interestingly, the *RRM2B* gene is amplified in various cancer types resulting in its

overexpression and poor patient prognosis [29]. In ccRCC samples, the overexpression of *RRM2B* is weak. In the TCGA dataset, in high grade tumors, the downregulation of *RRM2B* can be observed, in fact indicating that *RRM2B* may not be crucial in ccRCC development, in contrast to other cancer types. *RRM2B* is required for proper kidney function and its mutation in the mice model leads to renal failure [30].

Additionally, the deletion of *RRM2B* in mice caused defects in mitochondrial metabolism in renal tubules [31]. The kidney is physiologically hypoxic [32], and RRM2B together with RRM1 in RNR is capable to maintain the activity in hypoxic conditions as RRM2B is identified as a hypoxia-specific RNR subunit [33]. This all together may likely explain why in ccRCC, the RRM2B is neither amplified nor overexpressed as it occurs in other cancer types. Kidneys are more suitable for hypoxic conditions, and therefore RRM2B is crucial for their proper function, however, for ccRCC development, the RRM2 seems to be more relevant.

Furthermore, the comparative analysis revealed that expression levels of both *RRM1* and *RRM2* genes depend on mutation in the *PBRM1* gene encoding the BAF180 subunit of the SWI/SNF chromatin remodeling complex. Counterintuitive, the presence of WT form of BAF180 correlated with higher *RRM1* and *RRM2* overexpression, although it may be explained in the context of current literature data by the occurrence of SWI/SNF complex de-regulation in ccRCC and other cancer types [7, 25, 34-36].

We found direct binding of BAF180 to *RRM1* and *RRM2* promoter regions. Interestingly, the strongest binding of BAF180 to the *RRM1* promoter region correlated with H3 occupancy and enhanced trimethylated H3K27me3 around TSS1/TSS2. Thus, we cannot exclude that the observed expression of *RRM1* in ccRCC may result from the utilization of an alternative transcription start site (TSS2). Of note, the BAF180 target site in the *RRM1* promoter covers the target regions for various transcription factors, which have been reported as the interacting partners for SWI/SNF CRCs.

BAF180 directly binds the *RRM2* gene promoter region ~-610 bp before TSS1 and close to TSS2. In the human *RRM2* gene, there are two alternative TSS that generate alternative *RRM2* transcripts. Oppositely to *RRM1*, the BAF180 binding on *RRM2 locus* correlated with H3 and H3K14Ac enrichment around the -610 bp from TSS1 position suggesting the open chromatin status in this region and serving as an attractive explanation of observed high *RRM2* expression. The BAF180 binding regions were reported to be targeted also by the following transcription factors-known partners of SWI/SNF CRCs. Collectively, our results indicate the existence of differential regulatory functions for BAF180 on *RRM1* and *RRM2 loci*, however, the exact mechanism of BAF180 action on these *loci* still needs to be elucidated.

RNR enzyme is involved in dNTPs production for DNA replication, which is accelerated in cancer cells. The precise and balanced inhibition of RNR subunits by targeted therapy may sensitize the cancer cells for other treatment strategies by reducing their proliferation rate. RRM2 is recognized now as a poor prognosis marker in various cancer types like oral squamous cell carcinoma [37], lung adenocarcinoma [38], liver cancer [39] and is overexpressed in triple negative breast cancer cells [40]. Currently, the combined therapy of RRM2 suppression with other anticancer drugs is under investigation [41].

In recent years, the blocking of immune checkpoints with antibody against PD-1/PD-L1 (programmed death-1 receptor and its ligand) immunotherapy has been introduced for advanced ccRCC treatment [42]. Although this treatment was well tolerated and the majority of patients responded, a certain group of PD-1/PD-L1 treated ccRCC patients did not respond, reflecting primary resistance or developed secondary resistance during treatment. Factors contributing to immunotherapy resistance include, among others, mutation rates and tumor microenvironment (TME) [43]. In the mouse model for melanoma, the loss of *pbrm1* sensitized cancer cells for $CD8^+$ T cell-mediated killing [44]. Furthermore, the *PBRM1* loss in ccRCC caused the alteration in tumor gene expression landscape, potentially influencing the immunotherapy responsiveness [45]. The

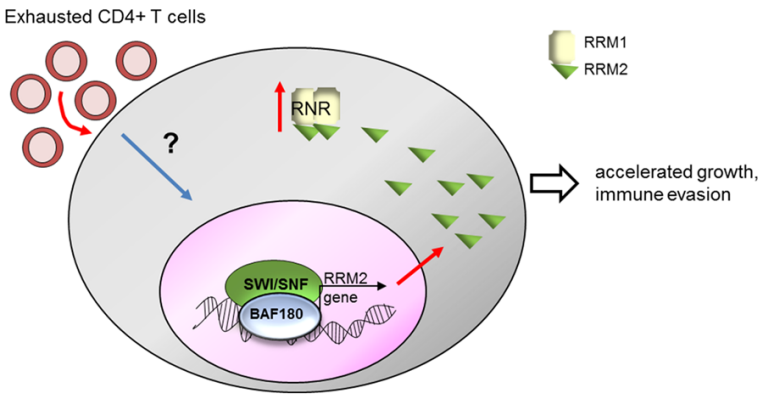

Figure 7. The regulation of RRM2 expression by BAF180 and SWI/SNF complex dependent on exhausting CD4⁺ T cells.

exact role of *PBRM1* mutation in immunotherapy response is still disputable, although available data indicated that *PBRM1* loss is associated with non-immunogenic tumor phenotype [46].

On the other hand, deficiency in BAF180 was correlated with reduction of CD4⁺ T cell number both in human and mouse ccRCC [47]. That observation is in consistency with our findings that wild type BAF180 is associated with a higher level of RRM2. *RRM2* expression in turn, correlates with expression of *CD4* and tumor infiltration by CD4⁺ T cells. Moreover, the presence of exhausting CD4⁺ T cells promotes an increased level of RRM2 protein in the 786-O cell line, suggesting that CD4⁺ TILs undergoing exhaustion may modulate TME and cancer gene transcription profile, possibly leading to immune evasion and acceleration of proliferation (**Figure 7**).

Therefore, the study presented here on the molecular regulation of *RRM* expression in ccRCC may serve as a solid basis for the development of new anticancer therapy targeting the RRM2 subunit of the RNR complex in combination with immunotherapy.

Acknowledgements

Polpharma Scientific Foundation Grant No. 5/XVII/18 (TJS), National Science Center Poland (NCN), UMO-2013/11/B/NZ2/00132 (JAS), UMO-2016/23/N/NZ1/01138 (IJ) and UMO-2017/25/N/NZ2/01909 (PC).

Disclosure of conflict of interest

None.

Address correspondence to: Elzbieta Sarnowska, Department of Experimental Immunotherapy, Maria Sklodowska-Curie National Research Institute of Oncology, Warsaw, Poland. Tel: +48-225-462782; E-mail: elasarn@coi.waw.pl; Tomasz J Sarnowski, Institute of Biochemistry and Biophysics, Polish Academy of Sciences, Warsaw, Poland. Tel: +48-604828940; E-mail: tsarn@ibb.waw.pl

References

[1] Manley BJ, Zabor EC, Casuscelli J, Tennenbaum DM, Redzematovic A, Becerra MF, Benfante-Manley BJ, Zabor EC, Casuscelli J, Tennenbaum DM, Redzematovic A, Becerra MF, Benfante N, Sato Y, Morikawa T, Kume H, Fukayama M, Homma Y, Ogawa S, Arcila ME, Voss MH, Feldman DR, Coleman JA, Reuter VE, Motzer RJ, Russo P, Hsieh JJ and Hakimi AA. Integration of recurrent somatic mutations with clinical outcomes: a pooled analysis of 1049 patients with clear cell renal cell carcinoma. Eur Urol Focus 2017; 3: 421-7.

[2] Swiatek M, Jancewicz I, Kluebsoongnoen J, Zub R, Maassen A, Kubala S, Udomkit A, Siedlecki JA, Sarnowski TJ and Sarnowska E. Various forms of HIF-1α protein characterize the clear cell renal cell carcinoma cell lines. IUBMB Life 2020; 1: 1-13.

[3] Harlander S, Schönenberger D, Toussaint NC, Prummer M, Catalano A, Brandt L, Moch H, Wild PJ and Frew IJ. Combined mutation in Vhl, Trp53 and Rb1 causes clear cell renal cell carcinoma in mice. Nat Med 2017; 23: 869-77.

[4] Muglia VF and Prando A. Renal cell carcinoma: histological classification and correlation with imaging findings. Radiol Bras 2015; 48: 166-74.

[5] Protzel C, Maruschke M and Hakenberg OW. Epidemiology, aetiology, and pathogenesis of renal cell carcinoma. Eur Urol Suppl 2012; 11: 52-9.

[6] Clark PE. The role of VHL in clear-cell renal cell carcinoma and its relation to targeted therapy. Kidney Int 2009; 76: 939-45.

[7] Sarnowska E, Szymanski M, Rusetska N, Ligaj M, Jancewicz I, Cwiek P, Skrodzka M, Leszczynski M, Szarkowska J, Chrzan A, Stachowiak M, Steciuk J, Maassen A, Galek L, Demkow T, Siedlecki JA and Sarnowski TJ. Evaluation of the role of downregulation of SNF5/INI1 core subunit of SWI/SNF complex in clear cell renal cell carcinoma development. Am J Cancer Res 2017; 7: 2275-89.

[8] Nargund AM, Pham CG, Dong Y, Wang PI, Osmangeyoglu HU, Xie Y, Aras O, Han S, Oyama T, Takeda S, Ray CE, Dong Z, Berge M, Hakimi AA, Monette S, Lekaye CL, Koutcher JA, Leslie CS, Creighton CJ, Weinhold N, Lee W, Tickoo SK, Wang Z, Cheng EH and Hsieh JJ. The SWI/SNF protein PBRM1 restrains VHL-loss-driven clear cell renal cell carcinoma. Cell Rep 2017; 18: 2893-906.

[9] Sarnowska E, Gratkowska DM, Sacharowski SP, Cwiek P, Tohge T, Fernie AR, Siedlecki JA, Koncz C and Sarnowski TJ. The role of SWI/SNF chromatin remodeling complexes in hormone crosstalk. Trends Plant Sci 2016; 21: 594-608.

[10] Jancewicz I, Siedlecki JA, Sarnowski TJ and Sarnowska E. BRM: the core ATPase subunit of SWI/SNF chromatin-remodelling complex-a tumour suppressor or tumour-promoting factor? Exp Mol Med 2019; 12: 1-17.

[11] Wei W, Lv Y, Gan Z, Zhang Y, Han X and Xu Z. Identification of key genes involved in the metastasis of clear cell renal cell carcinoma. Oncol Lett 2019; 17: 4321-8.

[12] Kolberg M, Strand KR, Graff P and Andersson KK. Structure, function, and mechanism of ribonucleotide reductases. Biochim Biophys Acta 2004; 1699: 1-34.

[13] Nordlund P and Reichard P. Ribonucleotide reductases. Annu Rev Biochem 2006; 75: 681-706.

[14] Stubbe JA, Nocera DG, Yee CS and Chang MC. Radical initiation in the class I ribonucleotide reductase: long-range proton-coupled electron transfer? Chem Rev 2003; 103: 2167-201.

[15] Bester AC, Roniger M, Oren YS, Im MM, Sarni D, Bensimon A, Zamir G, Shewach DS and Kerem B. Stages of cancer development. Cell 2013; 145: 435-46.

[16] Burrell RA, McGranahan N, Bartek J and Swanton C. The causes and consequences of genetic heterogeneity in cancer evolution. Nature 2013; 501: 338-45.

[17] D'angiolella V, Donato V, Forrester FM, Jeong Y-T, Pellacani C, Kudo Y, Saraf A, Florens L, Washburn MP and Pagano M. The cyclin F-ribonucleotide reductase M2 axis controls genome integrity and DNA repair. Cell 2012; 149: 1023-34.

[18] Zou Y, Zhou J, Xu B, Li W and Wang Z. Ribonucleotide reductase subunit M2 as a novel target for clear-cell renal cell carcinoma. Onco Targets Ther 2019; 12: 3267-75.

[19] Gumz ML, Zou H, Kreinest PA, Childs AC, Belmonte LS, LeGrand SN, Wu KJ, Luxon BA, Sinha M, Parker AS, Sun LZ, Ahlquist DA, Wood CG and Copland JA. Secreted frizzled-related protein 1 loss contributes to tumor phenotype of clear cell renal cell carcinoma. Clin Cancer Res 2007; 13: 4740-9.

[20] Peña-Llopis S, Vega-Rubín-de-Celis S, Liao A, Leng N, Pavía-Jiménez A, Wang S, Yamasaki T, Zhrebker L, Sivanand S, Spence P, Kinch L, Hambuch T, Jain S, Lotan Y, Margulis V, Sagalowsky AI, Summerour PB, Kabbani W, Wong SWW, Grishin N, Laurent M, Xie X, Haudenschild CD, Ross MT, Bentley DR, Kapur P and Brugarolas J. The SWI/SNF protein PBRM1 restrains VHL-loss-driven clear cell renal cell carcinoma. Cell Rep 2017; 18: 2893-906.

[21] Aguirre-Gamboa R, Gomez-Rueda H, Martínez-Ledesma E, Martínez-Torteya A, Chacolla-Huaringa R, Rodriguez-Barrientos A, Tamez-Peña JG and Treviño V. SurvExpress: an online biomarker validation tool and database for cancer gene expression data using survival analysis. PLoS One 2013; 8: e74250.

[22] Komata M, Katou Y, Tanaka H, Nakato R, Shirahige K and Bando M. Chromatin immunoprecipitation protocol for mammalian cells. Methods Mol Biol 2014; 1164: 33-8.

[23] Schmittgen TD and Livak KJ. Analyzing real-time PCR data by the comparative CT method. Nat Protoc 2008; 3: 1101-8.

[24] Jancewicz I, Szarkowska J, Konopinski R, Stachowiak M, Swiatek M, Blachnio K, Kubala S, Oksinska P, Cwiek P, Rusetska N, Tupalska A, Zeber-Lubecka N, Grabowska E, Swiderska B, Malinowska A, Mikula M, Jagielska B, Walewski J, Siedlecki JA, Sarnowski TJ, Markowicz S and Sarnowska EA. PD-L1 overexpression, SWI/SNF complex deregulation, and profound transcriptomic changes characterize cancer-dependent exhaustion of persistently activated CD4+ T cells. Cancers (Basel) 2021; 13: 4148.

[25] Cancer Genome Atlas Research Network. Comprehensive molecular characterization of clear cell renal cell carcinoma. Nature 2013; 499: 43-9.

[26] Gudbjartsson T, Hardarson S, Petursdottir V, Thoroddsen A, Magnusson J and Einarsson GV. Histological subtyping and nuclear grading of renal cell carcinoma and their implications for survival: a retrospective nation-wide study of 629 patients. Eur Urol 2005; 48: 593-600.

[27] Harte MT, O'Brien GJ, Ryan NM, Gorski JJ, Savage KI, Crawford NT, Mullan PB and Harkin DP. BRD7, a subunit of SWI/SNF complexes, binds directly to BRCA1 and regulates BRCA1-dependent transcription. Cancer Res 2010; 70: 2538-47.

[28] Yu X, Li Z and Shen J. BRD7: a novel tumor suppressor gene in different cancers. Am J Transl Res 2016; 8: 742-8.

[29] Iqbal W, Demidova EV, Serrao S, ValizadehAslani T, Rosen G and Arora S. RRM2B is fre-

quently amplified across multiple tumor types: implications for DNA repair, cellular survival, and cancer therapy. Front Genet 2021; 12: 628758.
[30] Kimura T, Takeda S, Sagiya Y, Gotoh M, Nakamura Y and Arakawa H. Impaired function of p53R2 in Rrm2b-null mice causes severe renal failure through attenuation of dNTP pools. Nat Genet 2003; 34: 440-5.
[31] Chen YF, Lin IH, Guo YR, Chiu WJ, Wu MS, Jia W and Yen Y. Rrm2b deletion causes mitochondrial metabolic defects in renal tubules. Sci Reports 2019 91 2019; 9: 13238.
[32] Tanaka S, Tanaka T and Nangaku M. Hypoxia and hypoxia-inducible factors in chronic kidney disease. Ren Replace Ther 2016; 2: 1-8.
[33] Foskolou IP, Jorgensen C, Leszczynska KB, Olcina MM, Tarhonskaya H, Haisma B, D'Angiolella V, Myers WK, Domene C, Flashman E and Hammond EM. Ribonucleotide reductase requires subunit switching in hypoxia to maintain DNA replication. Mol Cell 2017; 66: 206-220, e9.
[34] de Cubas AA and Rathmell WK. Epigenetic modifiers: activities in renal cell carcinoma. Nat Rev Urol 2018; 15: 599-614.
[35] Shigetomi H, Oonogi A, Tsunemi T, Tanase Y, Yamada Y, Kajihara H, Yoshizawa Y, Furukawa N, Haruta S, Yoshida S, Sado T, Oi H and Kobayashi H. The role of components of the chromatin modification machinery in carcinogenesis of clear cell carcinoma of the ovary. Oncol Lett 2011; 2: 591-7.
[36] Stachowiak M, Szymanski M, Ornoch A, Jancewicz I, Rusetska N, Chrzan A, Demkow T, Siedlecki JA, Sarnowski TJ and Sarnowska E. SWI/SNF chromatin remodeling complex and glucose metabolism are deregulated in advanced bladder cancer. IUBMB Life 2020: 1175-1188.
[37] Wang S, Wang XL, Wu ZZ, Yang QC, Xiong HG, Xiao Y, Li H and Sun ZJ. Overexpression of RRM2 is related to poor prognosis in oral squamous cell carcinoma. Oral Dis 2021; 27: 204-14.
[38] Jin CY, Du L, Nuerlan AH, Wang XL, Yang YW and Guo R. High expression of RRM2 as an independent predictive factor of poor prognosis in patients with lung adenocarcinoma. Aging (Albany NY) 2021; 13: 351-3535.
[39] Yang Y, Lin J, Guo S, Xue X, Wang Y, Qiu S, Cui J, Ma L, Zhang X and Wang J. RRM2 protects against ferroptosis and is a tumor biomarker for liver cancer. Cancer Cell Int 2020; 20: 587.
[40] Wilson EA, Sultana N, Shah KN, Elford HL and Faridi JS. Molecular targeting of RRM2, NF-κB, and Mutant TP53 for the treatment of triple-negative breast cancer. Mol Cancer Ther 2021; 20: 655-64.
[41] Zhan Y, Jiang L, Jin X, Ying S, Wu Z, Wang L, Yu W, Tong J, Zhang L, Lou Y and Qiu Y. Inhibiting RRM2 to enhance the anticancer activity of chemotherapy. Biomed Pharmacother 2021; 133: 110996.
[42] Kammerer-Jacquet SF, Deleuze A, Saout J, Mathieu R, Laguerre B, Verhoest G, Dugay F, Belaud-Rotureau MA, Bensalah K and Rioux-Leclercq N. Targeting the PD-1/PD-L1 pathway in renal cell carcinoma. Int J Mol Sci 2019; 20: 1692.
[43] Moreira M, Pobel C, Epaillard N, Simonaggio A, Oudard S and Vano YA. Resistance to cancer immunotherapy in metastatic renal cell carcinoma. Cancer Drug Resist 2020; 3: 454-71.
[44] Pan D, Kobayashi A, Jiang P, Andrade LF de, Tay RE, Luoma AM, Tsoucas D, Qiu X, Lim K, Rao P, Long HW, Yuan GC, Doench J, Brown M, Liu XS and Wucherpfennig KW. A major chromatin regulator determines resistance of tumor cells to T cell-mediated killing. Science 2018; 359: 770-5.
[45] Miao D, Margolis CA, Gao W, Voss MH, Li W, Martini DJ, Norton C, Bossé D, Wankowicz SM, Cullen D, Horak C, Wind-Rotolo M, Tracy A, Giannakis M, Hodi FS, Drake CG, Ball MW, Allaf ME, Snyder A, Hellmann MD, Ho T, Motzer RJ, Signoretti S, Kaelin WG, Choueiri TK and Van Allen EM. Genomic correlates of response to immune checkpoint therapies in clear cell renal cell carcinoma. Science 2018; 359: 801-6.
[46] Liu XD, Kong W, Peterson CB, McGrail DJ, Hoang A, Zhang X, Lam T, Pilie PG, Zhu H, Beckermann KE, Haake SM, Isgandrova S, Martinez-Moczygemba M, Sahni N, Tannir NM, Lin SY, Rathmell WK and Jonasch E. PBRM1 loss defines a nonimmunogenic tumor phenotype associated with checkpoint inhibitor resistance in renal carcinoma. Nat Commun 2020; 11: 2135.
[47] Aili A, Wen J, Xue L and Wang J. Mutational analysis of PBRM1 and significance of PBRM1 mutation in Anti-PD-1 immunotherapy of clear cell renal cell carcinoma. Front Oncol 2021; 11: 712765.